Original Article

Solute carrier family 16 member 1 as a potential prognostic factor for pancreatic ductal adenocarcinoma and its influence on tumor immunity

Meng Wang[1,2#], Lin Liu[1#], Xinze Li[1], Wenna Jiang[1], Jiawei Xiao[1], Qianhui Hao[1], Jiayi Wang[1], Abhinav V. Reddy[3], Alice Talbot[4], Shinichi Ikuta[5], Derun Tian[2,6], Li Ren[1]

[1]Department of Clinical Laboratory, Tianjin Medical University Cancer Institute and Hospital, National Clinical Research Center for Cancer, Key Laboratory of Cancer Prevention and Therapy, Tianjin, China; [2]Department of Clinical Laboratory Diagnostics, Tianjin Medical University, Tianjin, China; [3]Radiation Oncology, Northside Hospital, Atlanta, GA, USA; [4]Department of Oncology, St. John of God Hospital, Subiaco, WA, Australia; [5]Department of Surgery, Meiwa Hospital, Nishinomiya, Hyogo, Japan; [6]Department of Human Anatomy and Histology, Tianjin Medical University, Tianjin, China

Contributions: (I) Conception and design: L Ren, D Tian, M Wang; (II) Administrative support: L Ren; (III) Provision of study materials or patients: M Wang, L Liu, X Li; (IV) Collection and assembly of data: W Jiang, J Xiao; (V) Data analysis and interpretation: M Wang, Q Hao, J Wang; (VI) Manuscript writing: All authors; (VII) Final approval of manuscript: All authors.

[#]These authors contributed equally to this work.

Correspondence to: Derun Tian, PhD. Department of Clinical Laboratory Diagnostics, Tianjin Medical University, 1 Guangdong Rd, Tianjin 300203, China; Department of Human Anatomy and Histology, Tianjin Medical University, 22 Qixiangtai Rd, Tianjin 300070, China. Email: tiandr@tmu.edu.cn; Li Ren, PhD. Department of Clinical Laboratory, Tianjin Medical University Cancer Institute and Hospital, National Clinical Research Center for Cancer, Key Laboratory of Cancer Prevention and Therapy, West Huan-Hu Rd, Tianjin 300060, China. Email: liren@tmu.edu.cn.

Background: Solute carrier family 16 member 1 (*SLC16A1*) serves as a biomarker in numerous types of cancer. Tumor immune infiltration has drawn increasing attention in cancer progression and treatment. The objective of our study was to explore the association between *SLC16A1* and the tumor immune microenvironment in pancreatic ductal adenocarcinoma (PDAC).

Methods: Data were obtained from The Cancer Genome Atlas. The xCell web tool was used to calculate the proportion of immune cells according to *SLC16A1* expression. To further explore the mechanism of *SLC16A1*, immunity-related genes were screened from differentially expressed genes through weighted gene coexpression network analysis, examined via Gene Ontology and Kyoto Encyclopedia of Genes and Genomes analyses, and filtrated using univariate Cox regression and least absolute shrinkage and selection operator regression model combined correlation analysis ($P<0.05$). Next, CIBERSORT was used to analyze the correlation between immune cells and five important genes. *SLC16A1* expression and its clinical role in pancreatic cancer was clarified via immunohistochemical staining experiments. Finally, the effects of *SLC16A1* on the results of cancer immunity were evaluated by in vitro experiments.

Results: *SLC16A1* was overexpressed in PDAC tissues and could be an independent prognostic factor. *SLC16A1* was significantly negatively correlated with overall survival and suppressed the tumor immunity of PDAC. In clinic, *SLC16A1* expression was significantly positively correlated with tumor progression and poor prognosis. We also found that *SLC16A1* could suppress the antitumor ability of $CD8^+$ T cells.

Conclusions: *SLC16A1* is a biomarker for the prognosis of PDAC and can influence the immune environment of PDAC. These findings provide new insights into the treatment of PDAC.

Keywords: Pancreatic ductal adenocarcinoma (PDAC); solute carrier family 16 member 1; bioinformatics; tumor immunity; tumor microenvironment (TME)

Submitted Mar 05, 2024. Accepted for publication Apr 11, 2024. Published online Apr 28, 2024.
doi: 10.21037/jgo-24-147
View this article at: https://dx.doi.org/10.21037/jgo-24-147

Introduction

Pancreatic cancer is the seventh leading cause of cancer-related death worldwide, and pancreatic ductal adenocarcinoma (PDAC) is the most common type of pancreatic cancer, contributing to the death of more than 430,000 patients worldwide every year (1,2). It has an extremely poor prognosis, with the lowest reported 5-year overall survival (OS) rate among all malignant tumors from 2010–2016 (3). PDAC is predicted to be the second leading cause of cancer-related death by 2030 (4).

The poor prognosis of PDAC is likely due to the lack of early clinical symptoms, poor sensitivity of PDAC diagnostic tests, and lack of response to standard chemotherapeutic agents (5). Only 10–20% of patients with PDAC qualify for surgical resection due to the presence of distant metastases (6). Therefore, chemotherapy is recommended as first-line treatment to control progression in the majority of PDAC cases (7). For patients with advanced PDAC, multiagent chemotherapy is the standard of care with common regimens including FOLFIRINOX (folinic acid, fluorouracil, irinotecan hydrochloride, and oxaliplatin), gemcitabine/nab-paclitaxel, and nanoliposomal irinotecan/fluorouracil (7-9). Despite aggressive treatment, most patients eventually relapse (5). However, Options for treatment after first-line chemotherapy remain limited (10).

The role of immunotherapy in pancreatic cancer is largely unknown but it serves as an option for patients with poor response to conventional treatment (11-13). The limited benefit of immunotherapy may be related to the immunosuppressive tumor microenvironment (TME) of PDAC (14). As such, novel strategies are needed to improve the immunogenicity of PDAC. One potential target may be solute carrier family 16 member 1 (*SLC16A1*), which belongs to the monocarboxylate transporter family. The protein encoded by this gene is monocarboxylate transporter-1 (MCT1) which mediates lactate transportation (15,16). Increased *SLC16A1* expression contributes to tumor progression (17-20). In recent years, studies have found that *SLC16A1* still has implications for tumor immunity through regulating lactic acid metabolism (21,22).

Our study aimed to explore the clinical value and potential mechanism of *SLC16A1* in pancreatic cancer immunity. Using the bioinformatics method, we analyzed the transcriptome profiling data of PDAC from The Cancer Genome Atlas (TCGA) and explored the clinical significance of *SLC16A1* in PDAC. We divided patients into two groups according to their *SLC16A1* expression and compared their immune infiltration status. We then applied ESTIMATE and weighted gene coexpression network analysis (WGCNA) computational methods to screen for immune-related genes from differentially expressed genes (DEGs). We further investigated the underlying mechanism of *SLC16A1* by analyzing prognosis-related genes and examined their relationship with immune infiltration to provide new ideas for the clinical treatment of PDAC. We also validated the effect of *SLC16A1* on tumor progression and prognosis in patients with clinical samples. Finally, *in vitro* experiments indicated that the expression of *SLC16A1* in tumor cells could have an impact on $CD8^+$ T-cell function. In conclusion, we not only investigated the relationship between *SLC16A1* expression level and the prognosis of patients with tumors, but also revealed its impact on the immune microenvironment of tumor patients. We present this article in accordance with the TRIPOD reporting checklist (available at https://jgo.

Highlight box

Key findings

- Solute carrier family 16 member 1 (*SLC16A1*) was found to be an independent prognostic factor of pancreatic ductal adenocarcinoma (PDAC) and was closely correlated with tumor immunity.

What is known and what is new?

- Studies have revealed that *SLC16A1* is overexpressed in many kinds of cancers and that the upregulation of *SLC16A1* is associated with poor prognosis.
- We analyzed the relationship between *SLC16A1* and immune infiltration, identified relevant hub genes, and explored the impact of *SLC16A1* expression in tumor cells on immune cytotoxicity through *in vitro* experiments.

What is the implication, and what should change now?

- The study emphasized the critical role of *SLC16A1* in the prognosis of tumors and its potential as an immunotherapeutic target. However, the specific mechanism by which *SLC16A1* impacts the immune response of pancreatic cancer still requires further clarification.

amegroups.com/article/view/10.21037/jgo-24-147/rc).

Methods

Sample information

Data were obtained from TCGA dataset including PDAC samples [TCGA-PAAD (pancreatic adenocarcinoma), T] and normal pancreas samples (N). Transcriptome profiling data, survival data, and clinical information were downloaded from the University of California at Santa Cruz (UCSC) Xena browser (https://xena.ucsc.edu) (23).

Comparison of SLC16A1 expression between PDAC and normal tissues

Gene Expression Profiling Interactive Analysis (GEPIA; http://gepia.cancer-pku.cn/) is a multidimensional cancer genome dataset that integrates big data from TCGA and Genotype-Tissue Expression (GTEx) (24). In our study, differential expression analysis and survival analysis of *SLC16A1* were performed.

SLC16A1 expression was compared between PDAC and normal tissues by analyzing immunohistochemical (IHC) images from The Human Protein Atlas (https://www.proteinatlas.org) (25). The time-dependent receiver operating characteristic (ROC) curve (including 1-, 3-, and 5-year survival) was also examined using the R package "timeROC" (The Foundation of Statistical Computing) to reflect the sensitivity and specificity of *SLC16A1* (26).

Identification of DEGs

The R package "DESeq2" was used to identify DEGs between high *SLC16A1* expression (H-*SLC16A1*) and low expression (L-*SLC16A1*) groups according to the threshold of $|\log2 \text{ (fold change)}| > 1$ and a P value <0.05 (27). The R packages "Pheatmap", "ggpubr", and "ggthemes" were applied to generate heatmaps and volcano plots for the visualization of DEGs.

Immune infiltration analysis

We quantified stromal and immune scores using the ESTIMATE algorithm and evaluated the TME of each patient with PDAC and determined the stromal score (stromal content), immune score (extent of immune cell infiltration), ESTIMATE score (synthetic mark of stroma and immune), and tumor purity using R (28). Moreover, the "xCell" R package was used to calculate the proportion of immune cells relative to *SLC16A1* expression (29). CIBERSORT can accurately estimate the immune composition of tumor tissues and was thus used to analyze the correlation between immune cells and five important genes (30).

WGCNA of key modules according to immunoscore

WGCNA was performed on DEGs using the R package "WGCNA". Five modules were obtained, and their correlation with cluster, stromal score, immune score, ESTIMATE score, and tumor purity was calculated (31). The results showed that the brown module exhibited the highest correlation with immunoscore.

Enrichment analysis

For the analysis of the potential mechanism of genes in the brown module, Gene Ontology (GO) (32) and Kyoto Encyclopedia of Genes and Genomes (KEGG) analyses (33,34) were applied to understand the functions of genes of the brown module using the R package "clusterProfiler" (35).

Protein-protein interaction (PPI) network

Construction PPI networks were analyzed with the Search Tool for the Retrieval of Interacting Genes/Proteins (STRING) database (https://string-db.org/), and the results were visualized using Cytoscape (v. 3.7.2).

Prognostic modeling

Univariate Cox regression was used to screen the genes in the brown module related to survival, with P<0.01 used as the screening criterion. Subsequently, genes were selected and subjected to least absolute shrinkage and selection operator (LASSO) regression and further screen via Spearman correlation (P<0.05) to determine the most suitable genes (36).

Kaplan-Meier survival plots

The Kaplan-Meier survival plots of five important genes were analyzed via the Kaplan-Meier plotter portal (http://kmplot.com/analysis/) (37).

IHC staining

Fifty paraffin-embedded specimens confirmed to be pancreatic cancer were collected from the Tianjin Medical University Cancer Institute and Hospital. The study was conducted in accordance with the Declaration of Helsinki (as revised in 2013). The study was approved by the Ethics Committee of Tianjin Medical University Cancer Institute and Hospital (No. bc2023074) before the study began. We explained the necessary research procedures to all patients and obtained written informed consent for data and sample use. The tissues were incubated overnight with primary antibodies against SLC16A1 (20139-1-AP; Proteintech, Wuhan, China). After being washed three times with phosphate-buffered saline (PBS) for 15 min, the samples were incubated with secondary antibody at 37 ℃ for 60 min. After another washing, the specimens were stained with DAB and hematoxylin. Finally, the sections were observed under a microscope.

Western blot analysis

The cells were lysed in 10% sodium dodecyl-sulfate (SDS) containing 1% protease inhibitor (BL612A; Biosharp, Hefei, China), and the protein concentration was quantified via Bradford protein assay. A total of 10 μg of protein lysates from each sample was separated in 10% SDS–polyacrylamide gel electrophoresis (PAGE) and then transferred onto polyvinylidene fluoride membranes (IPVH00010; MilliporeSigma, Burling, MA, USA). After blocking was completed with 5% skim milk, the membranes were incubated overnight in a 4 ℃ refrigerator with the primary antibodies against SLC16A1 (20139-1-AP; Proteintech, Wuhan, China) and GAPDH (KM9002; Sungene Biotech, Tianjin, China). After being washed, the membranes were probed with anti-rabbit immunoglobin G (IgG) secondary antibody (ab205718; Abcam, Cambridge, UK) or anti-mouse IgG secondary antibody (ab6728; Abcam).

In vitro cytotoxicity assay for CD8⁺ T cells

Human pancreatic cancer cell lines (SW1990) were purchased from the American Type Culture Collection (ATCC; Manassas, VA, USA).

Cell transfection was performed using Lipofectamine 2000 (11668030, Invitrogen, Thermo Fisher Scientific, Waltham, MA, USA). To examine T-cell activation, peripheral blood mononuclear cells (PBMCs) and tumor cells were cocultured in RPMI-1640 medium supplemented with 10% fetal bovine serum (FBS; 04-001-1A; Biological Industries, Göttingen, Germany) and 0.01% penicillin/streptomycin. The cells were then incubated with KrO-conjugated anti-CD45 (B36294; Beckman Coulter, Brea, CA, USA), ECD-conjugated anti-CD3 (A07748; Beckman Coulter), A700-conjugated anti-CD8 (737659; Beckman Coulter), APC-conjugated anti-CD69 (A80711; Beckman Coulter), and PE-conjugated anti-programmed cell death protein 1 (PD-1; B30634; Beckman Coulter) at 25 ℃ for 30 min and analyzed via flow cytometry, data analyzed using FlowJo software (BD Biosciences).

After coculture, the $CD8^+$ T cells were isolated from PBMCs by $CD8^+$ T Cell Isolation Kit, human (130-094-156, Miltenyi Biotec, German) and cocultured again with SW1990 cells. The cytotoxicity of $CD8^+$ T cells was assessed using a lactate dehydrogenase (LDH) activity assay kit (BC0685; Solarbio, Beijing, China).

Statistical analysis

Univariate and multivariate Cox regression analyses were used to evaluate the significance of certain factors, including age, gender, tumor size, histological grade stage, lymph node metastasis, TNM stage, and *SLC16A1* expression. The χ^2 test was used to assess the statistical relationship between *SLC16A1* expression and other factors, including age, gender, tumor size, histological grade stage, lymph node metastasis, and TNM stage. All statistical analyses were run in R statistical software (v. 3.6.4) and SPSS statistical software (v. 25.0; IBM Corp., Armonk, NY, USA). $P<0.05$ indicated statistical significance.

Results

Prognostic value of SLC16A1

In general, the tumor tissues had higher *SLC16A1* expression than the normal tissues (*Figure 1A*). Moreover, IHC images of SLC16A1 antibody showed increased staining levels in PDAC tissues versus normal pancreatic tissues (*Figure 1B*), indicating the high protein expression in PDAC. Kaplan-Meier survival analysis showed that the H-*SLC16A1* group was associated with poorer OS compared with the L-*SLC16A1* group (*Figure 1C*). Univariate and multivariate Cox regression analyses suggested that *SLC16A1* may be an independent predictor

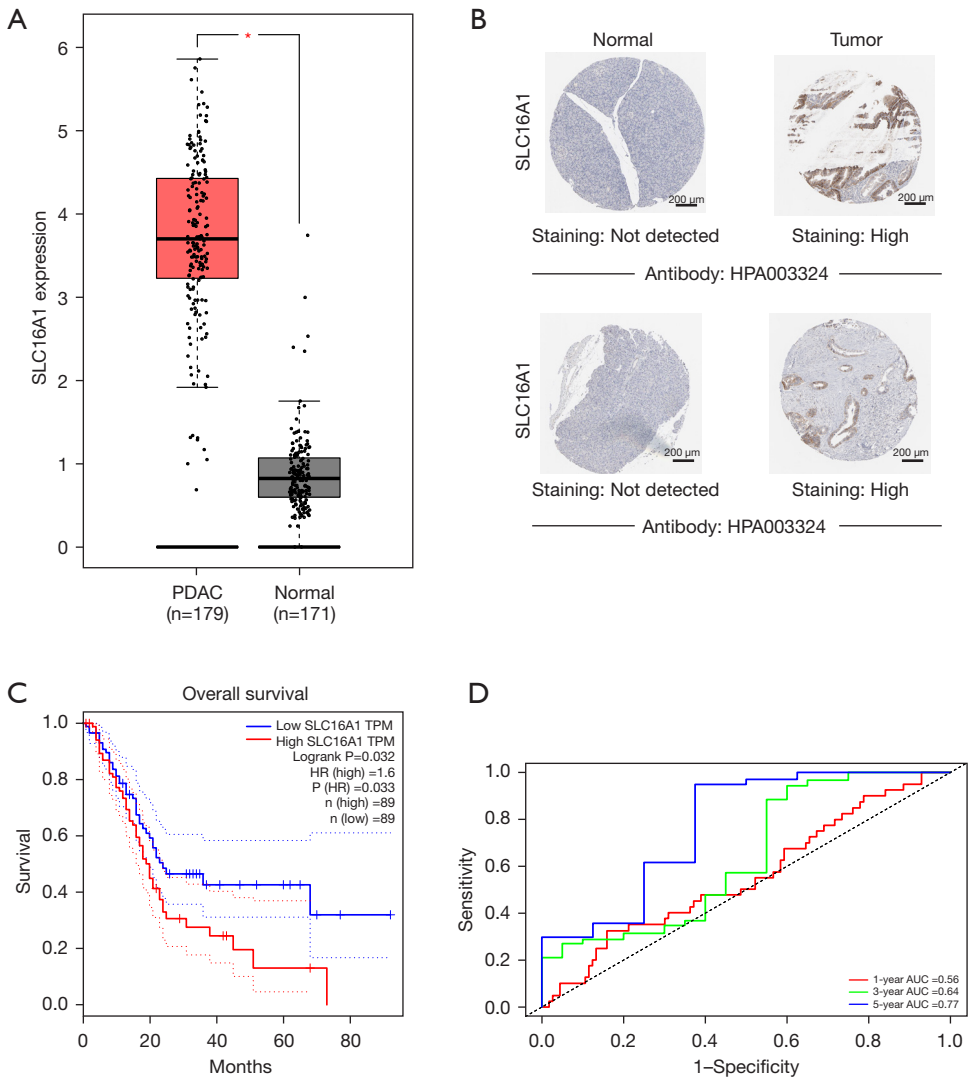

Figure 1 Prognostic value of SLC16A1 in PDAC. (A) Comparison of *SLC16A1* mRNA expression levels between PDAC and normal tissues. *, P<0.05. (B) Comparison of immunohistochemical images of SLC16A1 between tumor and normal tissues based on the Human Protein Atlas (tumor: https://www.proteinatlas.org/ENSG00000155380-SLC16A1/pathology/pancreatic+cancer#ihc; normal: https://www.proteinatlas.org/ENSG00000155380-SLC16A1/tissue/pancreas). (C) Kaplan-Meier survival analysis was performed to determine differences in overall survival between the H-*SLC16A1* and L-*SLC16A1* groups. (D) Time-dependent receiver operating characteristic curve analysis (including 1-, 3-, and 5-year survival) was performed to reflect the sensitivity and specificity of *SLC16A1*. *SLC16A1*, solute carrier family 16 member 1; PDAC, pancreatic ductal adenocarcinoma; TPM, transcripts per million; HR, hazard ratio; AUC, area under the curve.

of OS (*Table 1*). Reliability was determined via time-dependent ROC curves. The area under the curve (AUC) was 0.56, 0.64, and 0.77 for 1-, 3-, and 5-year survival, respectively, implying the good potential of *SLC16A1* in monitoring survival (*Figure 1D*). In summary, the findings strongly indicated that *SLC16A1* could be an independent prognostic factor for PDAC.

Identification of immune characteristics and immunity-related genes

To clarify the effect of *SLC16A1* on the TME, we examined the infiltration of immune cells in patients. The xCell results showed that *SLC16A1* expression was negatively correlated with many immune cells, including $CD8^+$ T cells and $CD4^+$ T cells (*Figure 2A*), suggesting the active immune

Table 1 Univariate and multivariate regression analyses of PDAC

Variable	Univariate analysis		Multivariate analysis	
	Hazard ratio (95% CI)	P value	Hazard ratio (95% CI)	P value
Age	1.03 (1.01–1.05)	0.01*	1.03 (1.00–1.05)	0.02*
Gender	1.28 (0.84–1.95)	0.24	1.20 (0.78–1.85)	0.40
Stage	1.23 (0.82–1.86)	0.31	0.79 (0.38–1.63)	0.52
Tumor size	1.49 (0.92–2.41)	0.10	1.26 (0.66–2.43)	0.48
LN metastasis	2.18 (1.28–3.71)	0.004*	1.93 (1.11–3.35)	0.02*
Histological grade	1.34 (1.00–1.80)	0.05	1.16 (0.85–1.59)	0.34
SLC16A1	1.39 (1.06–1.81)	0.01*	1.39 (1.03–1.87)	0.03*

Data are based on clinical information of patients in TCGA database. *, statistically significant at P<0.05. PDAC, pancreatic ductal adenocarcinoma; LN, lymph node; CI, confidence interval; TCGA, The Cancer Genome Atlas; *SLC16A1*, solute carrier family 16 member 1.

response of patients with low *SLC16A1* expression. In our search of immune-related genes, we obtained 1,203 DEGs (133 upregulated and 1,070 downregulated) between the two groups (H-*SLC16A1* and L-*SLC16A1*). The results were visualized using a heatmap (*Figure 2B*) and a volcano plot (*Figure 2C*). All DEGs were then considered for WGCNA (*Figure 2D*,*2E*) and divided into five modules (*Figure 2F*,*2G*), to reveal the association network between *SLC16A1* and DEGs. The brown module, which contained 140 immunity-related genes (*Figure 2H*), exhibited the highest correlation with immunoscore (Pearson correlation coefficient =0.86; P<0.0001) (*Figure 2I*).

Analysis of the potential mechanism of immunity-related genes

We performed GO (*Figure 3A*) and KEGG enrichment analyses (*Figure 3B*) to determine the biochemical functions of the key genes. From the GO terms, we found that these key genes had a close connection to immune processes, such as mononuclear cell differentiation, lymphocyte proliferation, and B-cell activation, which are key functions of immune infiltration. In the KEGG analysis, the pathways related to immunocytes, such as T-cell receptor signaling pathway and type 1 helper (Th1) and Th2 cell differentiation, were found to be significantly enriched.

Screening of prognostic genes

We conducted PPI analysis and assessed the correlations across the genes to further reveal the mechanism of *SLC16A1* in affecting immune infiltration (*Figure 4A*). Univariate Cox regression analysis was then performed on the DEGs from the expression matrices of patients to screen for potential prognostic genes. Factors (*BCL11A*, *CARMIL2*, *SEPT1*, *LINGO3*, *SCN4A*, *AFF3*, *OCM*, and *SPINK2*) with P<0.01 were sorted out for LASSO Cox regression analysis to identify robust markers (*Figure 4B*). A prognostic model containing six genes (*BCL11A*, *LINGO3*, *SCN4A*, *AFF3*, *OCM*, and *SPINK2*) was then constructed to evaluate the disease outcome. We next screened parameters with the LASSO Cox regression model according to the coefficients of nine genes (*Figure 4C*). Cross-validation analysis revealed that the optimal λ was six (*Figure 4D*). A moderate efficacy was verified with an AUC of 0.69 from the ROC curve (*Figure 4E*). This prognostic model also showed that patients who died of PDAC had high risk scores (*Figure 4F*). The distribution and status of OS were then analyzed by ranking the risk scores (*Figure 4G-4H*). The results showed that the patients with high-risk scores were likely to be deceased. Except for *AFF3* (P>0.05) (*Figure 5A*), all of the genes (*BCL11A*, *LINGO3*, *SCN4A*, *OCM*, and *SPINK2*) had a significant correlation with *SLC16A1* expression (P<0.05) and were subjected to subsequent analysis (*Figure 5B-5F*).

Correlation of the five genes with the proportion of tumor-initiating cells (TICs)

Investigating the types of infiltrating immune cells in patients was necessary to further explore the correlation of the five prognostic-related genes with the immune

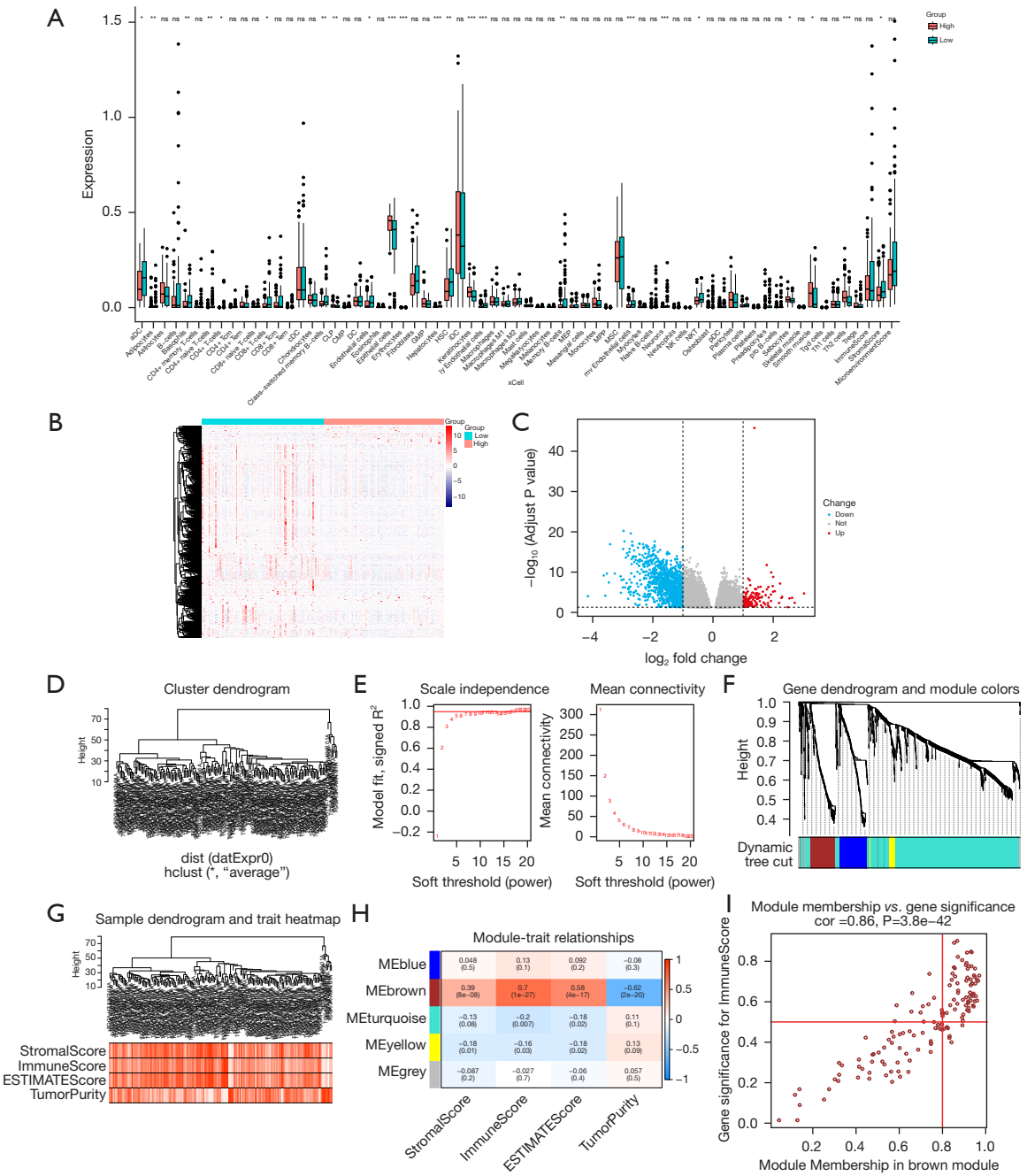

Figure 2 Screening for modules and genes related to immunity in DEGs. (A) Correlation of *SLC16A1* with immune cell infiltration. The blue and red floating bar plots represent the *SLC16A1* high- and low-expression groups, respectively. ns, P>0.05; *, P<0.05; **, P<0.01; ***, P<0.001. (B) Heatmap of DEGs between H-*SLC16A1* and L-*SLC16A1* in PDAC. (C) Volcano plot of DEGs between H-*SLC16A1* and L-*SLC16A1* in PDAC. (D) Sample clustering of PDAC. (E) Analysis of network topology for soft powers. (F) Dendrogram of all differentially expressed genes clustered based on the measurement of dissimilarity (1-TOM) and divided into five modules. (G) Clustering dendrogram of samples and the trait heatmap of ESTIMATE results. (H) Correlation heatmap between module eigengenes and ESTIMATE results. (I) Scatter plot of the brown module eigengenes. *SLC16A1*, solute carrier family 16 member 1; DEGs, differentially expressed genes; PDAC, pancreatic ductal adenocarcinoma; TOM, topological overlapmatrix; DC, dendritic cell; aDC, activated dendritic cell; cDC, classical dendritic cell; CLP, common lymphoid progenitor; CMP, common myeloid progenitor; GMP, granulocyte-macrophage progenitor; HSC, hematopoietic stem cell; iDC, immature dendritic cell; MEP, megakaryocyte-erythroid progenitor; MPP, multipotent progenitor; MSC, mesenchymal stem cell; pDC, plasmacytoid dendritic cells.

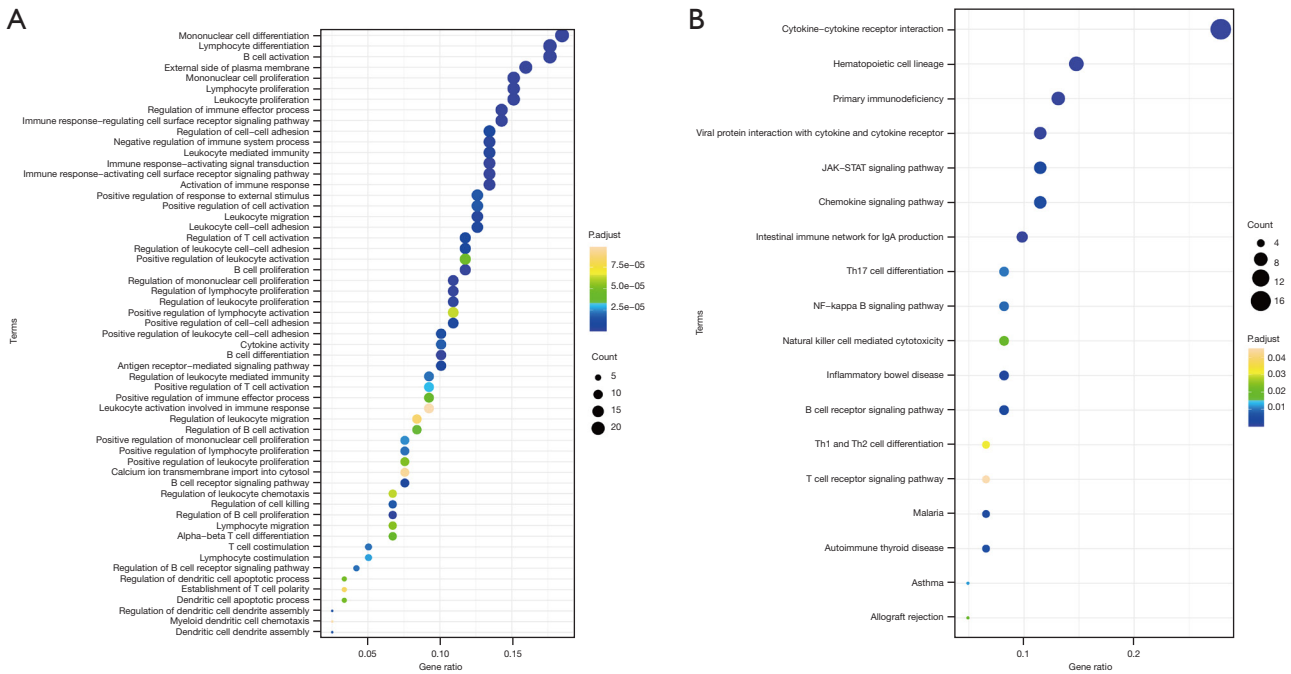

Figure 3 Potential mechanisms of immunity-related genes. (A) GO analysis of the brown module eigengenes; (B) KEGG analysis of the brown module eigengenes. GO, Gene Ontology; KEGG, Kyoto Encyclopedia of Genes and Genomes; JAK-STAT, Janus kinase/signal transducer and activator of transcription.

microenvironment. Hence, CIBERSORT was adopted for the evaluation of the relative proportion of 22 types of immune cells in all PDAC specimens (*Figure 6A*). The correlation between TICs and the expression of the five genes was confirmed (*Figure 6B*). The results suggested that the expression of five genes was positively correlated with the infiltration levels of naïve B cells, memory B cells, $CD8^+$ T cells, and activated $CD4^+$ memory T cells. Therefore, these five genes (*BCL11A*, *LINGO3*, *SCN4A*, *OCM*, and *SPINK2*) might be responsible for the preservation of the immune-active status in the TME. In addition, Kaplan-Meier survival analysis of OS also indicated that patients with a high expression of these genes had better prognosis (*Figure 6C*).

The clinical role of SLC16A1

Based on the bioinformatics method, we confirmed the key role of *SLC16A1* in human pancreatic cancer. The overexpression of *SLC16A1* was significantly associated with poor prognosis and the immunosuppressive phenotype in the TME. To evaluate the clinical significance of *SLC16A1*, we performed IHC staining in 50 clinical samples. We found that patients with a high expression of SLC16A1 in primary cancer tissues were associated with poorer OS and recurrence-free survival (RFS) (*Figure 7A*,*7B*). Univariate and multivariate Cox regression analyses also suggested that SLC16A1 could be an independent prognostic indicator of OS and recurrence-free survival (*Tables 2*,*3*). Furthermore, we analyzed the relationship between SLC16A1 and clinical parameters, including age, gender, tumor size, histological grade stage, lymph node metastasis, and TNM stage. SLC16A1 expression was significantly higher in patients with an advanced histological grade stage, TNM stage, and lymph node metastasis (*Table 4*).

SLC16A1 suppression of $CD8^+$ T-cell activity

To examine the correlation between the expression of SLC16A1 and tumor immunity, we increased the expression of SLC16A1 in the SW1990 human pancreatic cancer cell line (*Figure 8A*). Subsequently, we established a coculture model using SW1990 cells and PBMCs to investigate the impact of tumors on immune cells. Through *in vitro* LDH release assay, we confirmed that the overexpression of SLC16A1 could impair the cytotoxic effect of $CD8^+$ T cells

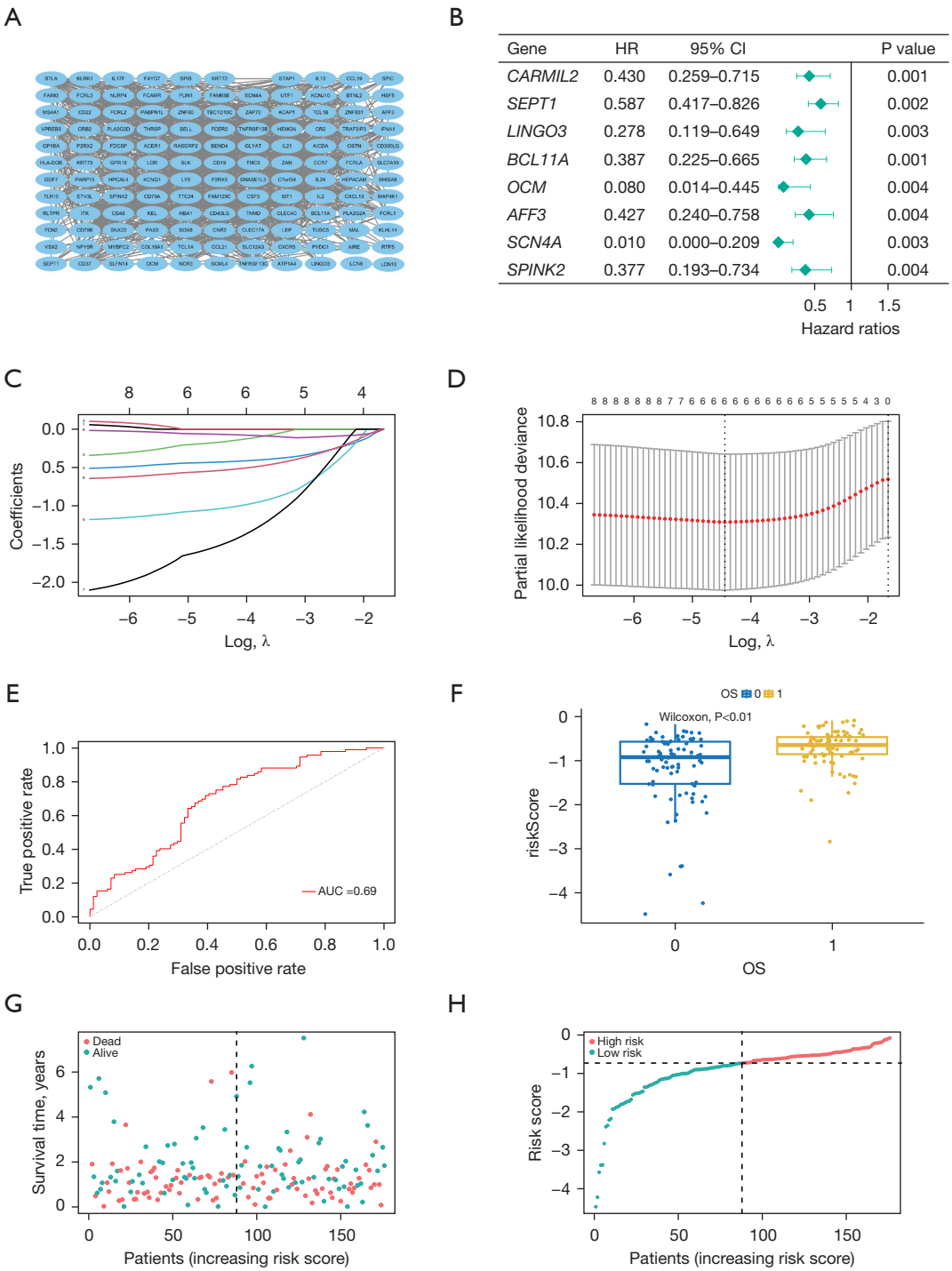

Figure 4 Screening of prognostic genes. (A) PPI network. (B) Univariate Cox regression analysis (P<0.01). (C) The variation characteristics of the coefficient of variables. (D) The optimum value of the parameter λ in the LASSO regression model as determined via cross-validation. (E) ROC curves for the prognostic risk model. (F) Box plot of risk scores (0: survival, 1: death). (G) Scatter plot distribution of survival time. (H) Scatter plot of risk scores from low to high. PPI, protein-protein interaction; LASSO, least absolute shrinkage and selection operator; ROC, receiver operating characteristic; HR, hazard ratio; CI, confidence interval; *SLC16A1*, solute carrier family 16 member 1; OS, overall survival.

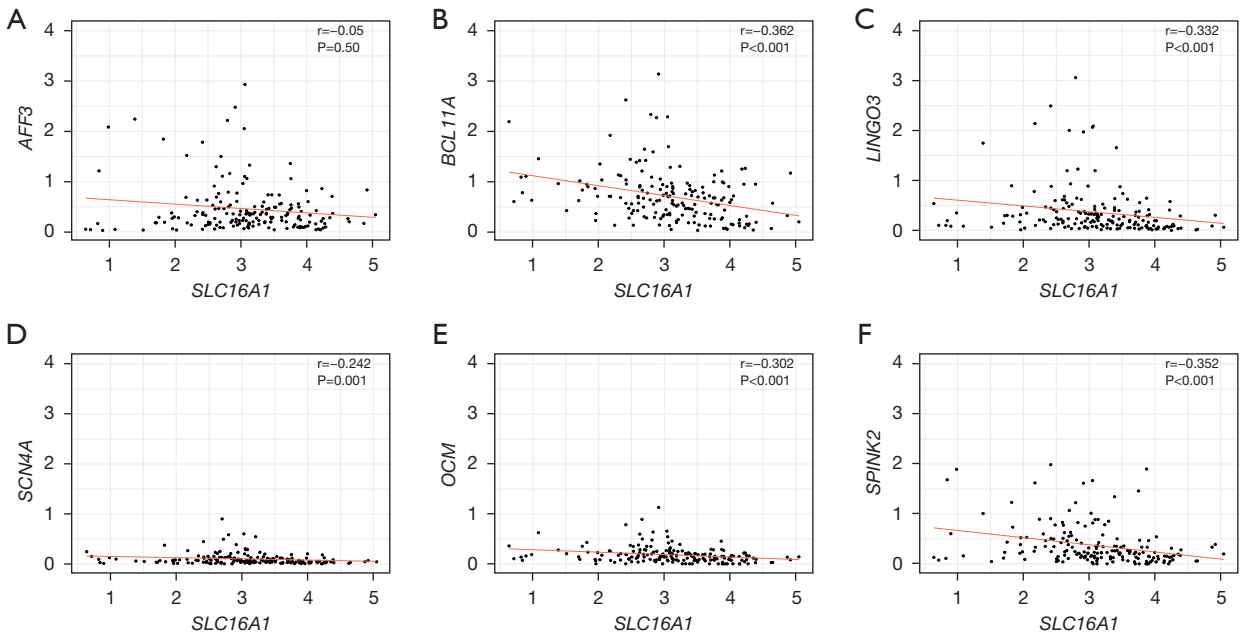

Figure 5 Correlation of *SLC16A1* expression with the prognostic genes Spearman correlation coefficient was used to analyze the correlation of *SLC16A1* with *AFF3* (A), *BCL11A* (B), *LINGO3* (C), *SCN4A* (D), *OCM* (E), and *SPINK2* (F).

in PBMCs against tumor cells (*Figure 8B*). Flow cytometry further revealed a reduction in CD69 expression on the surface of $CD8^+$ T cells from PBMCs cocultured with SLC16A1-overexpressed tumor cells (*Figure 8C*), while the population of exhausted $PD\text{-}1^+$ $CD8^+$ T cells remained relatively unchanged (*Figure 8D*). These findings confirmed that the overexpression of SLC16A1 in PDAC detrimentally affects the *in vitro* activation and tumor-killing capabilities of $CD8^+$ T cells.

Discussion

Our study suggests that *SLC16A1* is expressed at high levels in pancreatic cancer and has a significant negative correlation with the prognosis of PDAC. In addition, we also discussed the effect on TME. *SLC16A1* overexpression has been reported in many kinds of cancers, including brain cancer, breast cancer, ovarian cancer, melanoma, and cervical cancer (38-40). It is associated with tumor progression and promotes cancer cell migration and invasion. In cervical carcinoma, induced *SLC16A1* and CD147 expression was found to promote cancer cell migration (41). Payen *et al.* (19) also reported that *SLC16A1* independently promotes cancer cell migration and invasion.

Evidence indicates that there is a close correlation between tumor-infiltrating immune cells and cancer progression (42-44). Immunotherapy has been widely recognized as a form of therapy for many cancers, but it is controversial in PDAC (45-47). The limited efficacy of immunotherapy in PDAC may be attributed to its hypoxic and immunosuppressive TME. To improve sensitivity to immunotherapy, novel strategies are required to overcome this immunosuppressive TME. Strategies involving vaccines and stereotactic body radiotherapy have been investigated (48). One potential target is SLC16A1, which when overexpressed suppresses cytotoxic $CD8^+$ T cell activity. In fact, a study has shown that SLC16A1 inhibitors suppress tumor cell proliferation by decreasing lactate transport (49). However, clinical studies are warranted to further evaluate the efficacy of these inhibitors. In exploring the mechanism underlying *SLC16A1* impairment of tumor immune infiltration, we detected 1,203 DEGs between the H-*SLC16A1* and L-*SLC16A1* groups. We then performed WGCNA to identify the DEGs related to immune score and divided them into five modules. We concluded that the brown module exhibited the highest correlation with the immunoscore. According to the GO and KEGG enrichment analyses of the WGCNA-selected module eigengenes, the

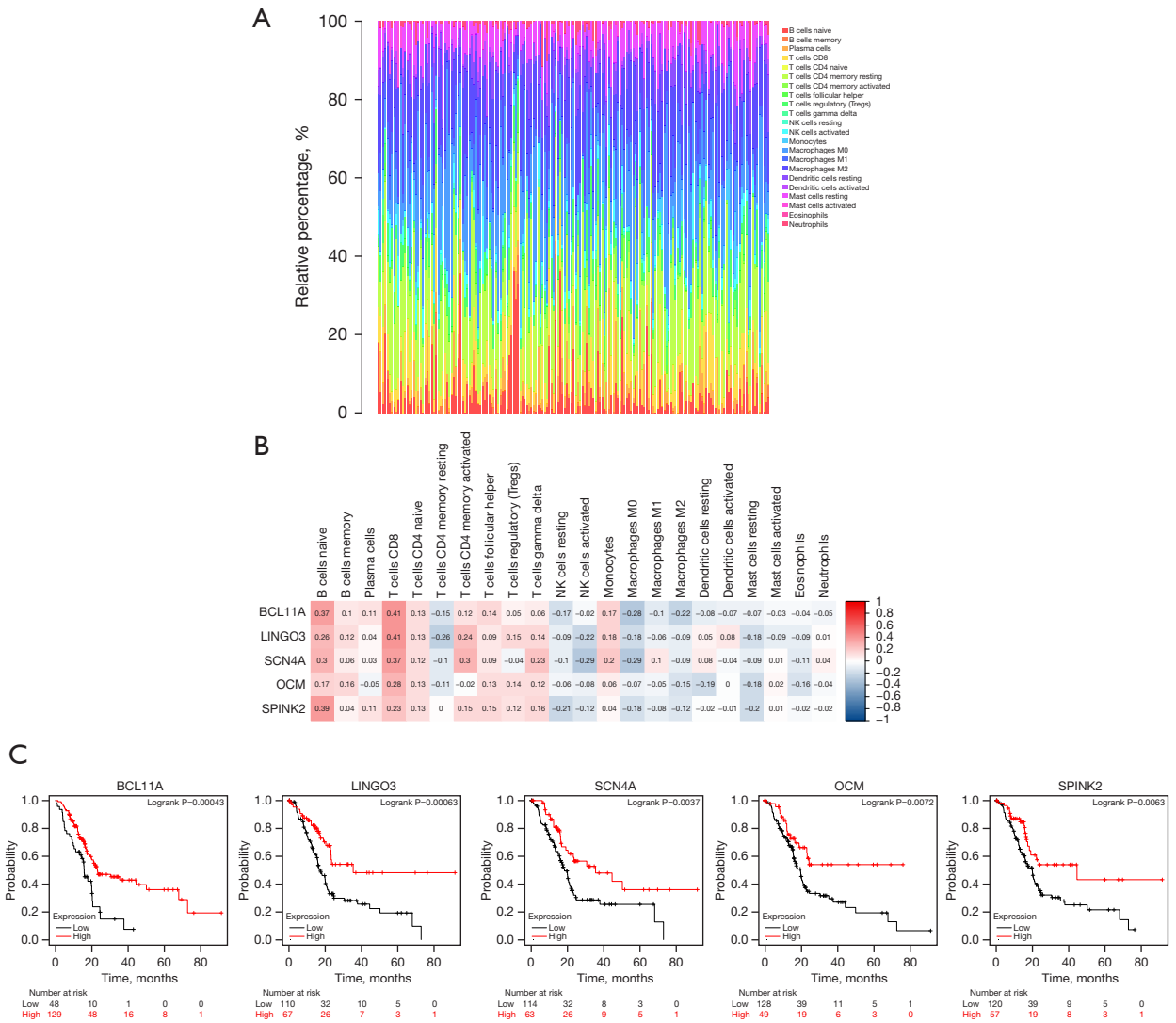

Figure 6 Correlation of the five genes with the proportion of TICs. (A) Bar plot showing the proportion of 22 kinds of immune cells in PDAC tumor samples. (B) Heatmap showing the correlation between immune cells and the five important genes. (C) Kaplan-Meier survival analysis was performed to determine difference in OS between the high-expression and low-expression groups. TICs, tumor-initiating cells; PDAC, pancreatic ductal adenocarcinoma; OS, overall survival.

genes of the brown module were closely related to immune infiltration processes, such as lymphocyte differentiation, lymphocyte proliferation, lymphocyte migration, and Th1 and Th2 cell differentiation.

We then attempted to identify immunoscore-related genes that contribute to survival. We applied Cox regression analysis and the LASSO regression model and identified six prognosis-related genes. By combining these results with the *SLC16A1* correlation findings, we ultimately obtained five important genes (*BCL11A*, *LINGO3*, *SCN4A*, *OCM*, and *SPINK2*) to further investigating the relationship between *SLC16A1* and tumor immunity by identifying potential target genes it might regulate. Correlations tests revealed that the expression of these important genes was negatively correlated with *SLC16A1*. To explore the effect on immune cell infiltration in tumors, we further adopted CIBERSORT for evaluating the relative proportion of immune cells in each PDAC specimen. As expected, B cells, memory B cells, $CD8^+$ T cells, and activated CD4 memory T cells showed a positive correlation with patient survival

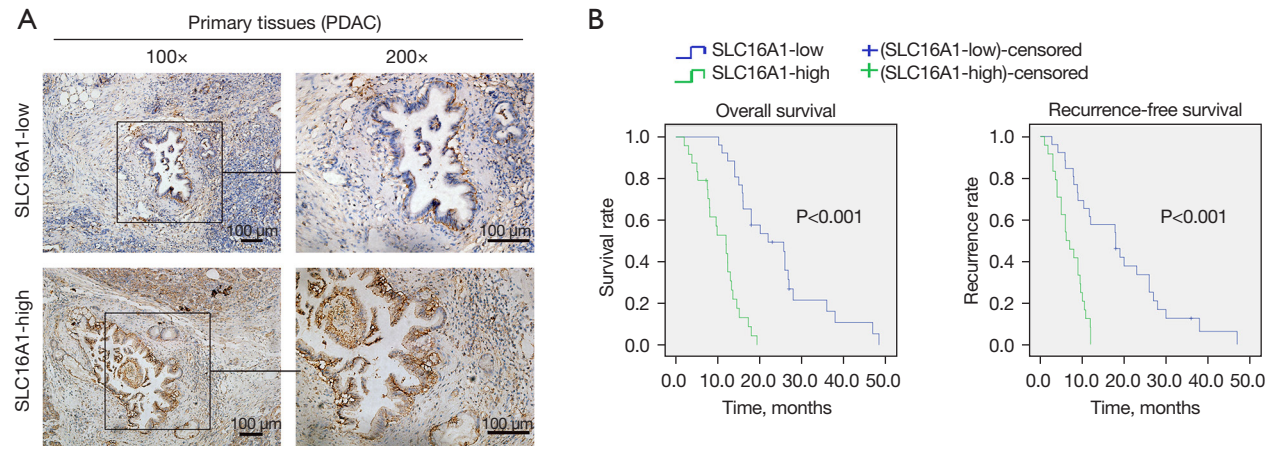

Figure 7 The clinical role of SLC16A1. (A) The expression of SLC16A1 in pancreatic cancer tissues was determined via immunohistochemistry. (B) Kaplan-Meier curves for overall survival and recurrence-free survival in patients with pancreatic cancer according to the expression of SLC16A1 in tumor tissues. SLC16A1, solute carrier family 16 member 1; PDAC, pancreatic ductal adenocarcinoma.

Table 2 Univariate Cox proportional hazards analysis of clinicopathological factors and SLC16A1 expression for overall survival and recurrence-free survival

Univariate analysis	Overall survival			Recurrence-free survival		
	HR	95% CI	P	HR	95% CI	P
Age	1.079	0.590–1.974	0.80	0.694	0.382–1.261	0.23
Gender	1.002	0.552–1.818	0.99	1.151	0.646–2.050	0.63
Tumor size	2.072	1.093–3.925	0.02*	1.845	1.006–3.382	0.04*
Histological grade	1.895	1.045–3.436	0.03*	1.890	1.057–3.379	0.03*
LN metastasis	1.805	0.994–3.277	0.05	1.662	0.924–2.989	0.09
TNM	1.912	1.01–3.591	0.04*	2.496	1.295–4.812	0.006*
SLC16A1 expression	6.741	3.168–14.347	<0.001*	4.877	2.319–10.257	<0.001*

Data are based on tissue IHC assay. Univariate Cox proportional hazard analysis was used for backward model selection. *, statistically significant at P<0.05. LN, lymph node; HR, hazard ratio; CI, confidence interval; IHC, immunohistochemistry; TNM, postoperatively tumor node metastasis; SLC16A1, solute carrier family 16 member 1.

Table 3 Multivariate Cox proportional hazards analysis of clinicopathological factors and SLC16A1 expression for overall survival and recurrence-free survival

Multivariate analysis	Overall survival			Recurrence-free survival		
	HR	95% CI	P	HR	95% CI	P
Tumor size	2.119	1.073–4.186	0.03*	1.563	0.816–2.992	0.17
Histological grade	1.525	0.821–2.831	0.18	1.360	0.729–2.539	0.33
TNM	1.180	0.536–2.601	0.68	1.964	0.937–4.116	0.07
SLC16A1 expression	5.832	2.450–13.883	<0.001	3.229	1.418–7.351	0.005*

*, statistically significant at P<0.05. HR, hazard ratio; CI, confidence interval; TNM, postoperatively tumor node metastasis; SLC16A1, solute carrier family 16 member 1.

Table 4 Correlation of tissue SLC16A1 expression and clinicopathological parameters

Parameter	SLC16A1 (n)		χ^2	P	r
	Low	High			
Age (years)			0.263	0.41	0.073
≤60	17	14			
>60	9	10			
Gender			0.349	0.38	–0.084
Male	13	14			
Female	13	10			
Tumor size (cm^3)			2.424	0.10	0.220
≤3.5	12	6			
>3.5	14	18			
Histological grade			9.641	0.002*	0.439
G1/G2	19	7			
G3	7	17			
LN metastasis			6.464	0.01*	0.360
N0	20	10			
N1	6	14			
TNM stage			9.507	0.002*	0.436
I	14	3			
II	12	21			

*, statistically significant at P<0.05. SLC16A1, solute carrier family 16 member 1; LN, lymph node; TNM, postoperatively tumor node metastasis.

(50-52). The potential of *SLC16A1* being an independent prognostic factor was verified by clinical samples. Through *in vitro* study, we found that overexpression of *SLC16A1* could weaken $CD8^+$ T-cell activity and impair the killing effect on pancreatic cancer cells. Therefore, *SLC16A1* may play an important role in the suppression of tumor immunity and subsequent resistance to immunotherapy. However, some potential limitations of our study still include: first, the size of the patient cohort or the number of samples used for certain analyses may impact the statistical power and generalizability of the results and the study has not analyzed all clinical prognostic factors, such as CA19-9 values. While the study provides insights into the potential prognostic and therapeutic implications of *SLC16A1*, further validation in independent patient cohorts and functional studies will be necessary to confirm its clinical relevance.

Conclusions

We investigated the role of *SLC16A1* in pancreatic cancer through use of bioinformatics, clinical study, and *in vitro* experiments. *SLC16A1* was found to be an independent prognostic factor of PDAC and closely related to tumor immunity. Overall, *SLC16A1* has the potential to be a diagnostic and prognostic target for PDAC.

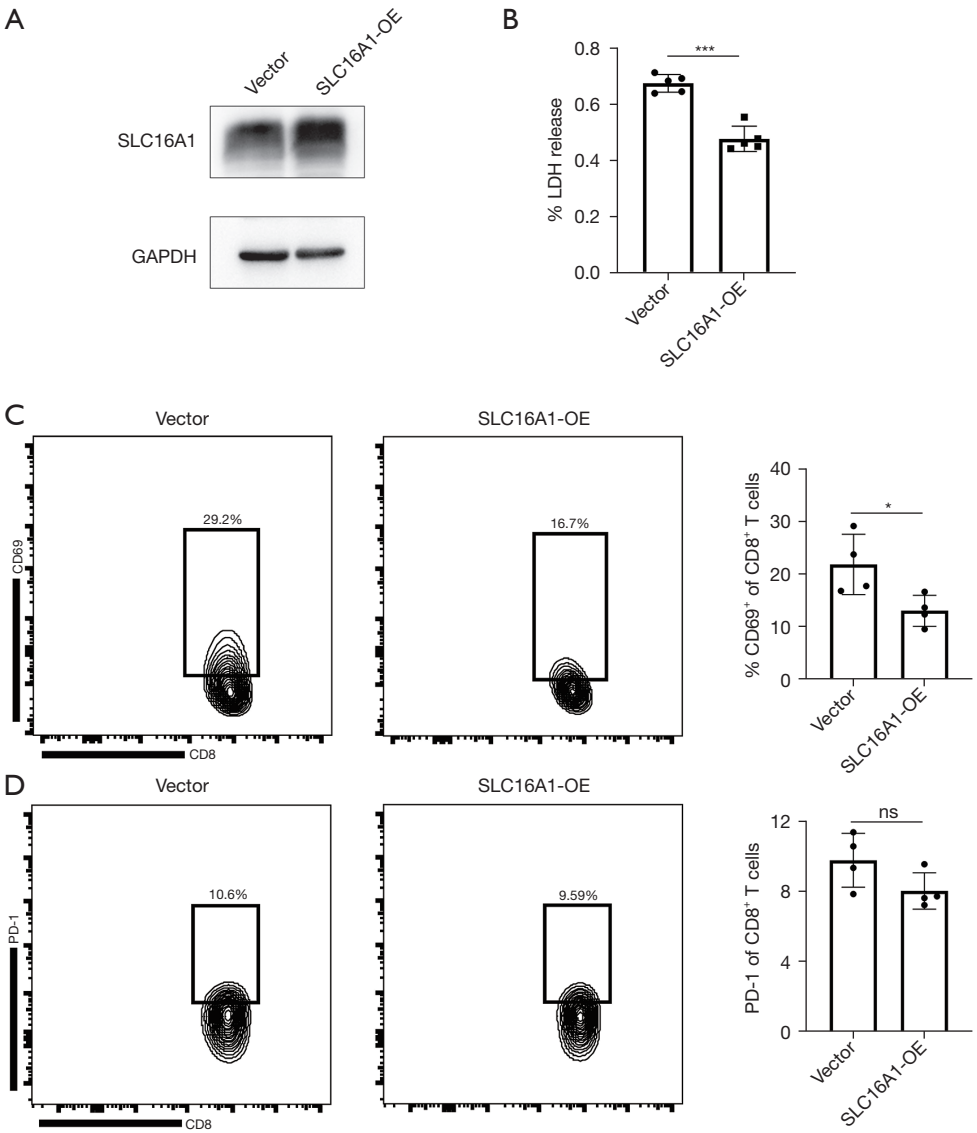

Figure 8 SLC16A1 suppression of CD8$^+$ T-cell activity. (A) Immunoblotting of SLC16A1 expression in Vector and SLC16A1-OE cells. (B) CD8$^+$ T cells in PBMCs were extracted using a CD8$^+$ T-cell purification kit and cocultured with tumor cells to determine the LDH release rate in the supernatant. (C,D) The positive rate of CD69 (C) and PD-1. (D) on CD8$^+$ T cells was detected after PBMCs were cocultured with tumor cells. ns, P>0.05; *, P<0.05; ***, P<0.001. OE, overexpression; PBMCs, peripheral blood mononuclear cells; LDH, lactate dehydrogenase; PD-1, programmed cell death protein; SLC16A1, solute carrier family 16 member 1.

Acknowledgments

We would like to thank all the patients for their important contributions and the administrators of the public databases for providing data.

Funding: This work was supported by the National Natural Science Foundation of China (grant No. 81802432).

Footnote

Reporting Checklist: The authors have completed the TRIPOD reporting checklist. Available at https://jgo.amegroups.com/article/view/10.21037/jgo-24-147/rc

Data Sharing Statement: Available at https://jgo.amegroups.

com/article/view/10.21037/jgo-24-147/dss

Peer Review File: Available at https://jgo.amegroups.com/article/view/10.21037/jgo-24-147/prf

Conflicts of Interest: All authors have completed the ICMJE uniform disclosure form (available at https://jgo.amegroups.com/article/view/10.21037/jgo-24-147/coif). The authors have no conflicts of interest to declare.

Ethical Statement: The authors are accountable for all aspects of the work in ensuring that questions related to the accuracy or integrity of any part of the work are appropriately investigated and resolved. The study was conducted in accordance with the Declaration of Helsinki (as revised in 2013). The study was approved by the Ethics Committee of Tianjin Medical University Cancer Institute and Hospital (No. bc2023074) before the study began. We explained the necessary research procedures to all patients and obtained written informed consent for data and sample use.

References

1. Rawla P, Sunkara T, Gaduputi V. Epidemiology of Pancreatic Cancer: Global Trends, Etiology and Risk Factors. World J Oncol 2019;10:10-27.
2. Halbrook CJ, Lyssiotis CA, Pasca di Magliano M, et al. Pancreatic cancer: Advances and challenges. Cell 2023;186:1729-54.
3. Sim W, Lim WM, Hii LW, et al. Targeting pancreatic cancer immune evasion by inhibiting histone deacetylases. World J Gastroenterol 2022;28:1934-45.
4. Rahib L, Smith BD, Aizenberg R, et al. Projecting cancer incidence and deaths to 2030: the unexpected burden of thyroid, liver, and pancreas cancers in the United States. Cancer Res 2014;74:2913-21.
5. Morrison AH, Byrne KT, Vonderheide RH. Immunotherapy and Prevention of Pancreatic Cancer. Trends Cancer 2018;4:418-28.
6. Strobel O, Neoptolemos J, Jäger D, et al. Optimizing the outcomes of pancreatic cancer surgery. Nat Rev Clin Oncol 2019;16:11-26.
7. Mizrahi JD, Surana R, Valle JW, et al. Pancreatic cancer. Lancet 2020;395:2008-20.
8. Zeng S, Pöttler M, Lan B, et al. Chemoresistance in Pancreatic Cancer. Int J Mol Sci 2019;20:4504.
9. Park W, Chawla A, O'Reilly EM. Pancreatic Cancer: A Review. JAMA 2021;326:851-62.
10. Fukahori M, Okabe Y, Shimokawa M, et al. Efficacy of second-line chemotherapy after treatment with gemcitabine plus nab-paclitaxel or FOLFIRINOX in patients with metastatic pancreatic cancer. Sci Rep 2023;13:19399.
11. Laface C, Memeo R, Maselli FM, et al. Immunotherapy and Pancreatic Cancer: A Lost Challenge? Life (Basel) 2023;13:1482.
12. Bear AS, Vonderheide RH, O'Hara MH. Challenges and Opportunities for Pancreatic Cancer Immunotherapy. Cancer Cell 2020;38:788-802.
13. Moral JA, Leung J, Rojas LA, et al. ILC2s amplify PD-1 blockade by activating tissue-specific cancer immunity. Nature 2020;579:130-5.
14. Erkan M, Hausmann S, Michalski CW, et al. The role of stroma in pancreatic cancer: diagnostic and therapeutic implications. Nat Rev Gastroenterol Hepatol 2012;9:454-67.
15. Halestrap AP. The SLC16 gene family - structure, role and regulation in health and disease. Mol Aspects Med 2013;34:337-49.
16. Silva A, Cerqueira MC, Rosa B, et al. Prognostic Value of Monocarboxylate Transporter 1 Overexpression in Cancer: A Systematic Review. Int J Mol Sci 2023;24:5141.
17. Zhang G, Zhang Y, Dong D, et al. MCT1 regulates aggressive and metabolic phenotypes in bladder cancer. J Cancer 2018;9:2492-501.
18. Pinheiro C, Penna V, Morais-Santos F, et al. Characterization of monocarboxylate transporters (MCTs) expression in soft tissue sarcomas: distinct prognostic impact of MCT1 sub-cellular localization. J Transl Med 2014;12:118.
19. Payen VL, Hsu MY, Rädecke KS, et al. Monocarboxylate Transporter MCT1 Promotes Tumor Metastasis Independently of Its Activity as a Lactate Transporter. Cancer Res 2017;77:5591-601.
20. Zhao Z, Wu MS, Zou C, et al. Downregulation of MCT1 inhibits tumor growth, metastasis and enhances

chemotherapeutic efficacy in osteosarcoma through regulation of the NF-κB pathway. Cancer Lett 2014;342:150-8.
21. Watson MJ, Vignali PDA, Mullett SJ, et al. Metabolic support of tumour-infiltrating regulatory T cells by lactic acid. Nature 2021;591:645-51.
22. Fischer K, Hoffmann P, Voelkl S, et al. Inhibitory effect of tumor cell-derived lactic acid on human T cells. Blood 2007;109:3812-9.
23. Haeussler M, Zweig AS, Tyner C, et al. The UCSC Genome Browser database: 2019 update. Nucleic Acids Res 2019;47:D853-8.
24. Tang Z, Li C, Kang B, et al. GEPIA: a web server for cancer and normal gene expression profiling and interactive analyses. Nucleic Acids Res 2017;45:W98-102.
25. Pontén F, Schwenk JM, Asplund A, et al. The Human Protein Atlas as a proteomic resource for biomarker discovery. J Intern Med 2011;270:428-46.
26. Heagerty PJ, Lumley T, Pepe MS. Time-dependent ROC curves for censored survival data and a diagnostic marker. Biometrics 2000;56:337-44.
27. Liu S, Wang Z, Zhu R, et al. Three Differential Expression Analysis Methods for RNA Sequencing: limma, EdgeR, DESeq2. J Vis Exp 2021;(175):e62528.
28. Yoshihara K, Shahmoradgoli M, Martínez E, et al. Inferring tumour purity and stromal and immune cell admixture from expression data. Nat Commun 2013;4:2612.
29. Aran D, Hu Z, Butte AJ. xCell: digitally portraying the tissue cellular heterogeneity landscape. Genome Biol 2017;18:220.
30. Chen B, Khodadoust MS, Liu CL, et al. Profiling Tumor Infiltrating Immune Cells with CIBERSORT. Methods Mol Biol 2018;1711:243-59.
31. Langfelder P, Horvath S. WGCNA: an R package for weighted correlation network analysis. BMC Bioinformatics 2008;9:559.
32. Ashburner M, Ball CA, Blake JA, et al. Gene ontology: tool for the unification of biology. The Gene Ontology Consortium. Nat Genet 2000;25:25-9.
33. Kanehisa M, Goto S, Furumichi M, et al. KEGG for representation and analysis of molecular networks involving diseases and drugs. Nucleic Acids Res 2010;38:D355-60.
34. Xu Q, Wang W, Hu H, et al. Screening of potential pain genes in pancreatic ductal adenocarcinoma (PDAC) based on bioinformatics methods. J Gastrointest Oncol 2023;14:420-8.
35. Yu G, Wang LG, Han Y, et al. clusterProfiler: an R package for comparing biological themes among gene clusters. OMICS 2012;16:284-7.
36. Peng Y, Liu C, Li M, et al. Identification of a prognostic and therapeutic immune signature associated with hepatocellular carcinoma. Cancer Cell Int 2021;21:98.
37. Nagy Á, Munkácsy G, Győrffy B. Pancancer survival analysis of cancer hallmark genes. Sci Rep 2021;11:6047.
38. Payen VL, Mina E, Van Hée VF, et al. Monocarboxylate transporters in cancer. Mol Metab 2020;33:48-66.
39. You S, Zhang J, Yu L, et al. Construction of SLC16A1/3 Targeted Gallic Acid-Iron-Embelin Nanoparticles for Regulating Glycolysis and Redox Pathways in Cervical Cancer. Mol Pharm 2023;20:4574-86.
40. Chatterjee P, Bhowmik D, Roy SS. A systemic analysis of monocarboxylate transporters in ovarian cancer and possible therapeutic interventions. Channels (Austin) 2023;17:2273008.
41. De Saedeleer CJ, Porporato PE, Copetti T, et al. Glucose deprivation increases monocarboxylate transporter 1 (MCT1) expression and MCT1-dependent tumor cell migration. Oncogene 2014;33:4060-8.
42. Bremnes RM, Busund LT, Kilvær TL, et al. The Role of Tumor-Infiltrating Lymphocytes in Development, Progression, and Prognosis of Non-Small Cell Lung Cancer. J Thorac Oncol 2016;11:789-800.
43. Seminerio I, Kindt N, Descamps G, et al. High infiltration of CD68+ macrophages is associated with poor prognoses of head and neck squamous cell carcinoma patients and is influenced by human papillomavirus. Oncotarget 2018;9:11046-59.
44. Zhu YH, Zheng JH, Jia QY, et al. Immunosuppression, immune escape, and immunotherapy in pancreatic cancer: focused on the tumor microenvironment. Cell Oncol (Dordr) 2023;46:17-48.
45. Banerjee K, Kumar S, Ross KA, et al. Emerging trends in the immunotherapy of pancreatic cancer. Cancer Lett 2018;417:35-46.
46. Henriksen A, Dyhl-Polk A, Chen I, et al. Checkpoint inhibitors in pancreatic cancer. Cancer Treat Rev 2019;78:17-30.
47. Sanmamed MF, Chen L. A Paradigm Shift in Cancer Immunotherapy: From Enhancement to Normalization. Cell 2019;176:677.
48. Parul A, Hanfei Q, Kabeer M, et al. Overall survival (OS) and pathologic response rate from a phase II clinical trial of neoadjuvant GVAX pancreas vaccine (with cyclophosphamide) in combination with nivolumab and

stereotactic body radiation therapy (SBRT) followed by definitive resection for patients with borderline resectable pancreatic adenocarcinoma (BR-PDAC). J Clin Oncol 2023;41:e16309.
49. Quanz M, Bender E, Kopitz C, et al. Preclinical Efficacy of the Novel Monocarboxylate Transporter 1 Inhibitor BAY-8002 and Associated Markers of Resistance. Mol Cancer Ther 2018;17:2285-96.
50. Speiser DE, Chijioke O, Schaeuble K, et al. CD4(+) T cells in cancer. Nat Cancer 2023;4:317-29.
51. Prokhnevska N, Cardenas MA, Valanparambil RM, et al. CD8(+) T cell activation in cancer comprises an initial activation phase in lymph nodes followed by effector differentiation within the tumor. Immunity 2023;56:107-124.e5.
52. Matsumoto H, Thike AA, Li H, et al. Increased CD4 and CD8-positive T cell infiltrate signifies good prognosis in a subset of triple-negative breast cancer. Breast Cancer Res Treat 2016;156:237-47.

Cite this article as: Wang M, Liu L, Li X, Jiang W, Xiao J, Hao Q, Wang J, Reddy AV, Talbot A, Ikuta S, Tian D, Ren L. Solute carrier family 16 member 1 as a potential prognostic factor for pancreatic ductal adenocarcinoma and its influence on tumor immunity. J Gastrointest Oncol 2024;15(2):730-746. doi: 10.21037/jgo-24-147

